THERMODYNAMIC STUDY AND ELECTROCHEMICAL INVESTIGATION OF CALCEIN AS CORROSION INHIBITOR FOR MILD STEEL IN HYDROCHLORIC ACID SOLUTION

DEMET ÖZKIR [a,b], EMEL BAYOL [a1], A. ALİ GÜRTEN [c], YAVUZ SÜRME [a]*

[a] *Niğde University, Faculty of Arts and Sciences, Department of Chemistry, 51240 Niğde, Turkey*
[b] *Niğde University, Ulukışla Vocational School,51900 Niğde, Turkey*
[c] *Osmaniye Korkut Ata University, Faculty of Arts and Sciences, Department of Chemistry, 80000 Osmaniye, Turkey*
(Accepted: April 25, 2012 - Accepted: November 20, 2013)

ABSTRACT

The corrosion behaviour of mild steel in 1.0 M HCl solution containing different concentrations of Calcein at different temperatures was investigated using the impedance, potentiodynamic polarization and linear polarization techniques. Long term tests were accomplished by hydrogen gas evolution and impedance measurements. The results showed that inhibition efficiency has increased with the inhibitor concentration and temperature increment. The adsorption of the inhibitor on the mild steel surface obeyed the Langmuir isotherm. Activation energy values at concentrations of Calcein were lower than that of uninhibited system. The thermodynamic parameters of adsorption deduced reveal a strong interaction of Calcein on the mild steel surface.

Keywords: Mild Steel; Polarization; EIS; Acid Corrosion; Calcein

1. INTRODUCTION

Mild steel is the most widely used engineering material such as metal-processing equipment, marine applications, nuclear and fossil fuel power plants, transportation, chemical processing, pipelines, mining, construction. It is usually exposed to strong acids especially HCl solutions between 5 %-15 % at temperature up to 80 °C in operations such as industrial acid cleaning, acid descaling and acid pickling in many different ways and for many reasons [1-5]. In such cases, the corrosion can be controlled by means of inhibitors in order to retard undesirable metal dissolution in acidic media. Inhibitors are chemical substances added to an acid solution to prevent corrosion or to decrease it at an acceptably low rate. They are used mainly in closed or circulating systems [6] and are selected for their effectiveness in protecting the specific metal or combination of metals in a given system. The corrosion of metals in aqueous solutions can be inhibited by a very wide range of organic substances, particularly those containing elements of group V and VI such as nitrogen, phosphorus, oxygen, and sulphur [2,4,7,8]. The efficiency of an organic compound depends on its ability to get adsorbed on the metal surface. The adsorption of these compounds is influenced by the electronic structure of inhibiting molecules, aromatic structure, steric factor, and electron density at donor site, presence of functional group, etc., molecular area and molecular weight of the inhibitor molecule [7,9].

The aim of this work is: *i)* to examine corrosion inhibition of mild steel in hydrochloric acid solutions by 2,2',2'',2'''-(3',6'-dihydroxy-3-oxo-3*H*-spiro[isobenzofuran-1,9'-xanthene]-(2',7'-diyl) bis(methylene) bis(azanetriyl) tetra acetic acid (Calcein) using the electrochemical impedance spectroscopy, potentiodynamic polarization and linear polarization techniques, *ii)* to observe the effect of long-term experiments such as open circuit potential and impedance measurements as a function of time on the inhibition efficiency and also, *iii)* to investigate the effect of temperature on the corrosion rate in order to calculate the thermodynamic parameters.

2. MATERIALS AND METHODS

2.1 Electrolyte and test solutions

Hydrochloric acid of analytical grade and distilled water were used in the preparation of aggressive media. The concentration of Calcein employed ranged from $1x10^{-5}$ to $1x10^{-3}$ mol/L in HCl solution. Chemical structure of Calcein is given in Fig 1. All solutions were prepared from analytical-grade chemical reagents in distilled water without further purification. For each experiment, freshly prepared solution was used under air atmosphere without stirring.

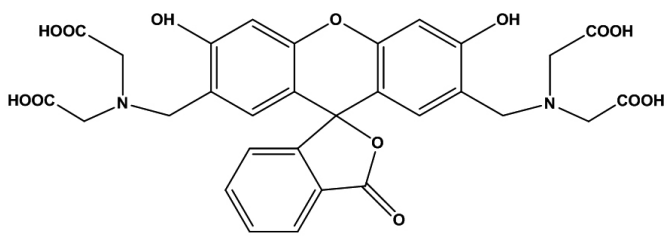

Figure 1: Chemical structure of Calcein.

2.2 Preparation of mild steel electrode

The corrosion tests were performed on mild steel specimens with a composition of (*wt.%*): C : 0.105, Si : 0.261, Mn : 0.694, P : 0.0206, S : 0.0310, Cr: 0.0471, Mo: 0.00347, Ni: 0.0575, Al: 0.00299, Co: 0.00400, Cu: 0.896, Nb: 0.00295, Ti: 0.00110, V: 0.0121, W: 0.00534 and the reminder iron. The mild steel sample was embedded in polyester, which had a surface area of 0.50 cm^2 that was in contact with the corrosive media. The specimen was polished successively with 150, 600 and 1200 grit emery papers, rinsed with distilled water and then with acetone and dried in air.

2.3 Hydrogen Evolution Measurements

A hydrogen gas evolution measurement was carried out with a burette filled with 1.0 M HCl solution and was up-turned over the working electrode. The initial volume of air in the burette was recorded at 293 K then the volume of hydrogen gas due to the corrosion reaction of mild steel in acid solution was measured for five days at every 24 hour. The same process was applied in the presence of Calcein concentrations from $1.0x10^{-5}$ M to $1.0x10^{-3}$ M.

2.4 Electrochemical measurements

Electrochemical experiments were carried out in a three electrode cell. The working electrode with a shape of a disc was cut from the mild steel sheet. A platinum electrode and an Ag/AgCl electrode were used as counter and reference electrodes, respectively. The temperature conditions were thermostatically controlled by using wear-jacketed cell. The electrochemical studies were performed by using a CHI 660B model electrochemical analyzer under computer control. The mild steel electrode was immersed in the solution for 60 min and a steady state open circuit potential (E_{corr}) was recorded. The polarization curves were performed by using potentiodynamic technique at -0.550 V cathodic potential and at +0.250 V (Ag/AgCl) anodic potential of corrosion potential at a scan rate of 1.0 mV s^{-1}. The experiments were conducted in two parts; the first reading was from the open-circuit corrosion potential to the cathodic side and the second was from open-circuit corrosion potential to the anodic side. Corrosion current density (i_{corr}) was determined by Tafel

e-mail: emelbayol@nigde.edu.tr

extrapolation of cathodic Tafel lines. To obtain linear polarization resistance, the mild steel was polarised to ±10 mV mV of the corrosion potential at a scan rate of 0.1 mV.s^{-1}. As a result, polarization resistance (R_{lpr}) values were calculated from the current potential plot. AC impedance measurements (*EIS*) were carried out at the open circuit potential (E_{corr}). The measurements were carried out with applied sinusoidal potential waves of 5 mV amplitudes, with frequencies ranging from 1x10^{5} Hz to 5x10^{-3} Hz. The AC impedance results were fitted by using the Zview software from Scribner Associates. All resistance and capacitance values given in tables and figures include the surface area of the working electrode as SI units.

2.5 UV-visible analysis

The UV-visible absorption spectra of 1.0 M HCl solution containing 1x10^{-5} M Calcein before and after immersion of the mild steel for 120 h were recorded by using Shimadzu model UV-160A spectrophotometer.

2.6 Surface morphological studies

The surface morphology of corroded mild steel specimens in the absence and presence of 1x10^{-5} M, 1x10^{-4} M and 1x10^{-3} M concentrations of Calcein after 120 h was studied using a Leon 440 scanning electron microscope.

3. RESULTS AND DISCUSSION

3.1 Potentiodynamic polarization measurements

Polarization curve for mild steel electrode at 293 K in 1.0 M HCl, in the absence and presence of Calcein at different concentrations are shown in Fig 2. As can be seen from the figure, the addition of inhibitor have caused a decrease in both cathodic and anodic currents proposing that the presence of Calcein reduces anodic dissolution and retards the hydrogen evolution reaction by blocking the active reaction sites on the metal surface [10].

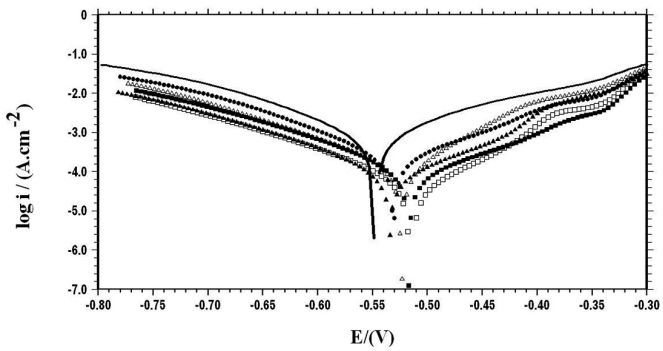

Figure 2: Polarization curves for the mild steel in 1.0 M HCl and containing different concentration of Calcein at 293 K (-1.0 M HCl, ● 1x10^{-5} M Calcein, Δ 5x10^{-5} M Calcein, ▲1x10^{-4} M Calcein, □ 5x10^{-4} M Calcein, ■ 1x10^{-3} M Calcein).

The electrochemical parameters such as, cathodic Tafel slopes (β_c), corrosion potential (E_{corr}), corrosion current density (i_{corr}), degree of surface coverage (θ) and the inhibition efficiency (*IE* %) values are listed in Table 1.

The corrosion current density (i_{corr}) was calculated from the cathodic polarization curves and the inhibition efficiency was calculated by the following formula [2]:

$$IE(\%) = \frac{i_{corr} - i'_{corr}}{i_{corr}} x100 \qquad (1)$$

where i_{corr} and i'_{corr} represent the corrosion current densities in the absence and presence of the Calcein respectively. Accordingly, inhibition efficiency values have reached to 87% when the concentration of Calcein has increased to 1.0x10^{-4} M and then remained constant as shown in Table 1.

The corrosion current value (i_{corr}) in an inhibitor free solution decreased from 822 μA/cm^2 to 104 μA/cm^2 at 1.0x10^{-4} M concentration of Calcein. The corrosion current density (i_{corr}) has decreased as Calcein concentrations have increased which indicates that this compound acts as inhibitor, and the degree of inhibition depends on the concentration. It is clear from Table 1 that there is a small shift towards anodic direction in the values of corrosion potential. Reports from literature [11] claims that, if the shift in E_{corr} *(i)* is >85 mV with respect to E_{cor}, the inhibitor can be seen as a cathodic or anodic type and *(ii)* if shift in E_{corr} is <85 mV, inhibitor can be seen as mixed type inhibitor. In our study maximum shift in E_{corr} value was 32 mV towards anodic direction, which indicates that this molecule could be classified as a mixed type inhibitor with predominantly control of anodic reaction in acidic solution [12, 13].

Table 1: Potentiodynamic polarization parameters for the corrosion of the mild steel by Calcein in 1.0 M HCl at 293 K.

Concentration (M)	E_{corr} (V/Ag/AgCl)	$-\beta_c$ (mV/dec)	i_{corr} (μA/cm^2)	θ	*IE* (%)
Blank	- 0.549	113	822	-	-
Calcein					
1x10^{-5}	- 0.532	103	244	0.70	70
5x10^{-5}	- 0.525	108	140	0.83	83
1x10^{-4}	- 0.534	112	104	0.87	87
5x10^{-4}	- 0.519	110	116	0.86	86
1x10^{-3}	- 0.517	114	116	0.86	86

The variable values of the cathodic Tafel slopes suggest that the inhibiting action of Calcein occurs by simple blocking of the electrode surface area, thus decreasing the surface area available for hydrogen evolution without affecting the reaction mechanism [6 ,14].

3.2. Electrochemical impedance spectroscopy and linear polarization resistance measurements

The corrosion behaviour of the mild steel in 1.0 M hydrochloric acid solution, in the absence and presence of Calcein, was investigated by using the electrochemical impedance spectroscopy technique at 293 K. The impedance parameters derived from Nyquist and Bode plots are given in Table 2 and plots are shown in Fig 3.

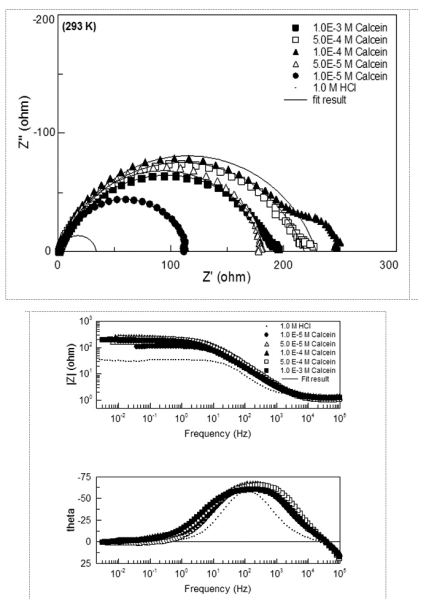

Figure 3: Nyquist and Bode diagrams of mild steel in 1.0 M HCl absence and presence of Calcein.

As can be seen from Fig 3, the Nyquist and Bode plots of mild steel in HCl solution does not yield perfect semicircle as expected from the theory of electrochemical impedance spectroscopy (Fig 3). The deviation from ideal semicircle is generally attributed to the frequency dispersion as well as to the inhomogeneities of surface and mass transport resistant [15,16]. The experimental impedance data were fitted according to the electrical equivalent circuit diagram given in Fig. 4a in order to model the uninhibited mild steel/ solution interface.

The difference in real impedance at lower and higher frequencies must be considered as polarization resistance (R_p). The polarization resistance includes charge transfer resistance (R_{ct}) which corresponds to resistance between the metal/outer Helmholtz plane and diffuse layer resistance (R_d) containing corrosion products and accumulated species *etc.* on the metal surface of the semi-ellipse model that has been reported by Erbil et al [17-19].

Nyquist plots showed two slightly disturbed capacitive loops (two time constants in Bode format); at high and low frequency regions in the presence of Calcein. The first loop that appeared at high frequency region is attributed to the R_{ct} and the R_d. Where, the sum of these resistances is known as pore resistance (R_{por}). The second loop is attributed to the film resistance and all of the other accumulated species such as corrosion products, inhibitor molecules, etc. The electrochemical equivalent circuit model employed for inhibited systems was presented in Fig 4b. The R_p value includes the R_{ct} value, which corresponds to metal dissolution within the pores of oxide film, the R_d against the diffusion of corrosive species through the pores and the oxide film resistance (R_f). This approach agrees very well with those reported by Solmaz et al [20].

Table 2: Data obtained from EIS spectra and linear polarization resistance for mild steel with Calcein in 1.0 M HCl at 293 K.

Concentration (M)	$-E_{corr}$ (V)	R_s (Ω)	R_p (Ω)	CPE		IE%	R_{lpr}(Ω)	*IE%
				Q(x10^{-6} s^n Ω^{-1})	α			
Blank	0.549	1.5	32.5	398	0.892	-	33	-
1.0x10^{-5}	0.532	1.2	115	261	0.840	72	107	69
5.0x10^{-5}	0.525	1.2	182	226	0.819	82	180	82
1.0x10^{-4}	0.534	1.3	248	182	0.837	87	226	86
5.0x10^{-4}	0.519	1.0	218	288	0.772	85	181	82
1.0x10^{-3}	0.517	1.2	190	343	0.761	83	206	84

*IE%: Determined from linear polarization resistance.

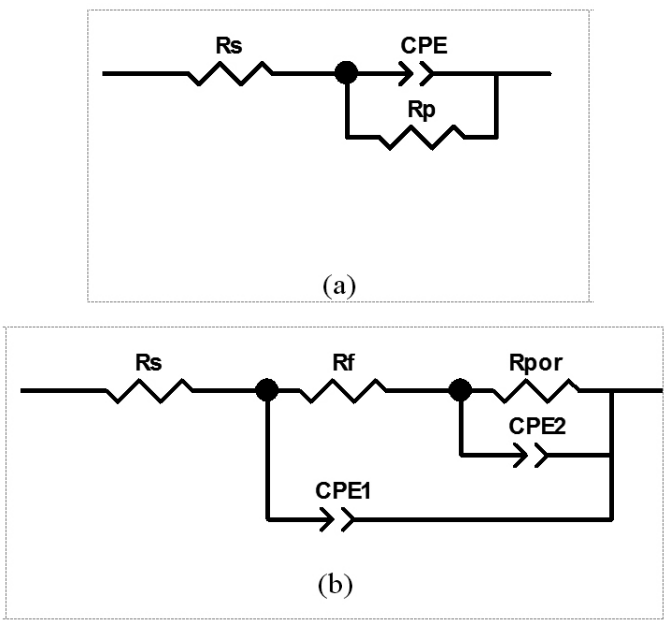

Figure 4: Equivalent circuit used to fit impedance spectra in Fig 3 in the absence (a) and presence (b) of Calcein. [(a) $R_p = R_{ct} + R_d + R_a$ for the diagram (b). $R_p = R_f + R_{por}$ ($R_{por} = R_{ct} + R_d + R_a$) for the diagram R_s: solution resistance, R_{ct}: charge transfer resistance, R_d: diffuse layer resistance, R_a: resistance of accumulated species at metal/solution interface, R_f: film resistance, R_{por}: pore resistance, CPE_1: film capacitance, CPE and CPE_2: double layer capacitance].

The high frequencies (HF) measurements are not in agreement with pure capacity behavior, indeed a constant-phase element (CPE) behavior is observed which could be associated to current and potential distributions due to surface heterogeneity or to continuously distributed time constants for charge-transfer reactions [21,22]. CPE represents all the frequency-dependent electrochemical phenomena; including double layer capacitances and diffusion processes [19,23]. In the case of a pure capacity, α = 1 value as slope should be obtained. The impedance expression of a CPE is:

$$Z_{CPE} = \frac{1}{Q(j\omega)^{\alpha}} \qquad (2)$$

where -α represents the slope of the straight line plotted Z_{im} versus frequency in both logarithmic coordinates at HF. Q is the CPE parameter corresponding to a capacitance when α = 1 and w is the pulsation (rad s^{-1}). *CPE* was used in place of the double layer capacitance in order to give a more accurate fit to the experimental result [24,25]. With the α value, Q was calculated from:

$$Q = \frac{\sin(\alpha\frac{\pi}{2})}{Z_{im}(2\pi f)^{\alpha}} \qquad (3)$$

The Q value can be plotted versus the frequency in logarithmic coordinates and a constant value is obtained at HF range which represents CPE coefficient [26].

The percentage inhibition efficiency, *IE* (%), was calculated by using the following expression

$$EI(\%) = \left(\frac{R_p - R^{o}{}_p}{R_p}\right)x100 \qquad (4)$$

where R_p and R^{o}_p are the polarization resistance of the electrode with and without inhibitor respectively. Table 2 summarizes, R_s, R_p, CPE and the exponential constant *(α)* that were calculated by using the Zview software from complex plane data.

The electrochemical impedance results clearly indicated that the increase in Calcein concentration has decreased the capacitance and increased polarization resistance and in the maximum phase angle, therefore a larger diameter of the semicircle was observed in Nyquist plots (Fig 3 and Table 2). The polarization resistance value of the blank was 32.5 Ω and has increased to 247.9 Ω when the concentration of Calcein added was 1.0x10^{-4} M. Meanwhile, the addition of Calcein has decreased the constant phase element values (Table 2). The decrease in the CPE values is due to the decrease in local dielectric constant and/or an increase in the thickness of the electrical double layer [27]. The increase in polarization resistance and the decrease of capacitance is attributed to the formation of a barrier layer of the inhibitor molecule on the metal surface [3,4].

The electrochemical parameters obtained from the linear polarization resistance (R_{lpr}) in 1.0 M HCl in the presence of Calcein are given in Table 2. The values of R_{lpr} have increased from 33 to 226 Ω at 1.0x10^{-4} M Calcein. The values of R_{lpr} remained constant at higher concentration of Calcein. The inhibition efficiency was calculated from the obtained polarization resistance values by using the following relationship:

$$EI(\%) = \left(\frac{R_{lpr} - R^{o}_{lpr}}{R_{lpr}} \right) x100 \qquad (5)$$

where R°_{lpr} and R_{lpr} are the polarization resistances in absence and in presence of inhibitor. As the concentration of Calcein has increased, the value of linear polarization resistance has also increased and consequently the inhibition efficiency has increased up to 86%. The values calculated from R_{lpr} measurements were in a good agreement with those of potentiodynamic polarization curves and impedance data.

3.3. Effect of immersion time on inhibition efficiency

Electrochemical impedance spectroscopy (*EIS*) is an in situ, non-destructive, rapid and convenient technique useful for evaluating the performance of organic-coated metals [28] and has been widely used with good results for investigation of protective properties of organic inhibitors on metals. More reliable results can be obtained from this technique, because it does not significantly disturb the double layer at the metal/solution interface [18]. Besides, *EIS* can also provide detailed information of the metal-inhibitor system.

The variation in inhibition efficiency of Calcein on the corrosion of mild steel in 1.0 M HCl at 293 K was studied for five concentrations at different immersion times. To eliminate confusion in the long-term tests, Nyquist diagrams for 24 and 120 hours have been given in Fig 5. However, Table 3 summarizes the polarization resistances derived from Nyquist plots.

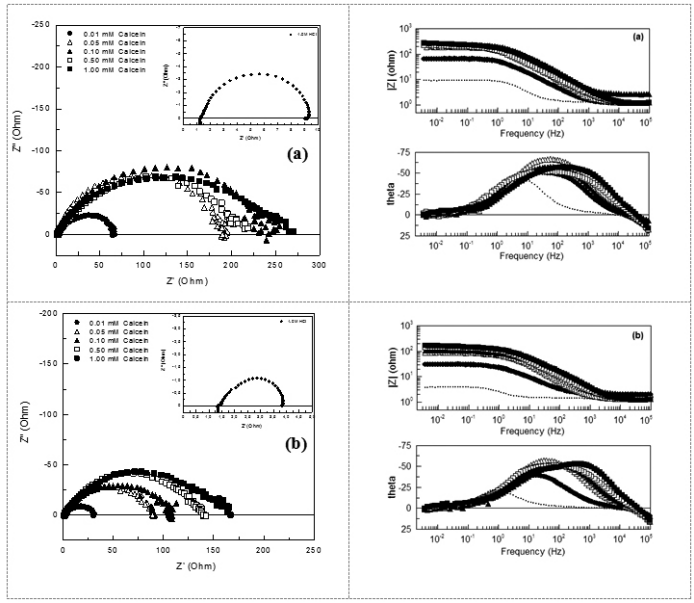

Figure 5: Nyquist and Bode plots of mild steel in 1.0 M HCl different containing concentrations of Calcein with time [(a) 24, (b) 120 hours].

Table 3: Polarization resistance and inhibition efficiency values of mild steel in 1.0 M HCl solution in the absence and presence of various concentrations Calcein after different immersion time.

Time/h	R_s	R_p	CPE		IE	Time/h	R_s	R_p	CPE		IE
4	(Ω)	(Ω)	**Q(x10^6 s^a Ω^{-1})**	**a**	**%**	**72**	(Ω)	(Ω)	**Q(x10^6 s^a Ω^{-1})**	α	**%**
Blank	1.5	26	1025	0.885	-	Blank	1.1	3.1	61463	0.855	-
Calcein						Calcein					
1x10^{-5}	1.2	145	341	0.864	82	1x10^{-5}	1.3	40	3653	0.727	92
5x10^{-5}	1.3	223	243	0.871	88	5x10^{-5}	1.6	107	965	0.794	97
1x10^{-4}	1.6	291	316	0.794	91	1x10^{-4}	1.1	141	584	0.763	98
5x10^{-4}	1.3	194	1183	0.690	87	5x10^{-4}	1.2	167	1301	0.684	98
1x10^{-3}	1.1	272	721	0.673	90	1x10^{-3}	1.0	198	661	0.701	98
24						**96**					
Blank	1.2	8.2	10404	0.885	-	Blank	1.3	2.6	88512	0.859	-
Calcein						Calcein					
1x10^{-5}	1.1	67	2314	0.732	88	1x10^{-5}	1.2	33	4578	0.717	92
5x10^{-5}	1.2	188	499	0.843	96	5x10^{-5}	1.3	92	1181	0.779	97
1x10^{-4}	2.5	237	468	0.772	96	1x10^{-4}	1.1	117	692	0.751	98
5x10^{-4}	1.1	214	1332	0.682	96	5x10^{-4}	1.2	148	1263	0.691	98
1x10^{-3}	1.1	265	440	0.616	97	1x10^{-3}	1.0	182	688	0.703	98
48						**120**					
Blank	1.3	3.7	35056	0.875	-	Blank	1.0	2.1	118040	0.834	-
Calcein						Calcein					
1x10^{-5}	1.3	53	2885	0.732	93	1x10^{-5}	1.9	29	5973	0.696	93
5x10^{-5}	1.3	133	768	0.809	97	5x10^{-5}	1.3	88	1344	0.768	98
1x10^{-4}	1.6	179	515	0.767	98	1x10^{-4}	1.9	103	928	0.714	98
5x10^{-4}	1.2	189	1354	0.680	98	5x10^{-4}	1.2	135	1239	0.696	98
1x10^{-3}	1.1	227	649	0.694	98	1x10^{-3}	1.1	153	826	0.684	99

The polarization resistance obtained in the absence and presence of Calcein that acts as a function of immersion time is given in Fig 5. From these plots, it is evident that at long period of immersion, the impedance response of mild steel in acidic solution decreases significantly and increases by increasing the concentrations of Calcein (Table 3). The calculated R_p values were plotted against time and are given in Fig 6. The results showed that the immersion time

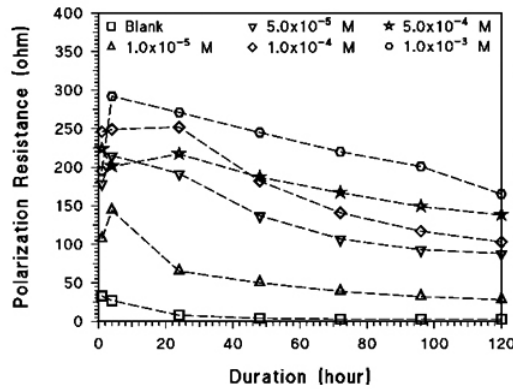

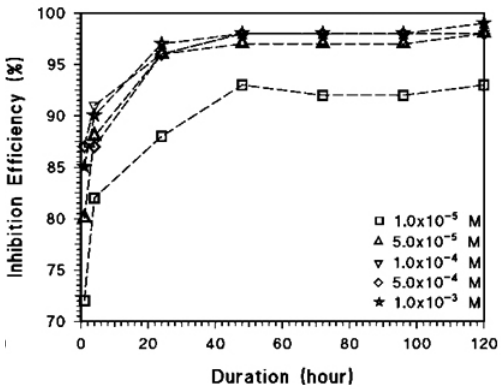

has increased inhibition efficiency values remarkably.

Figure 6: Polarization resistance (R_p) versus time and inhibition efficiency (IE) versus time plots of mild steel immersed in 1.0 M HCl containing Calcein.

As shown in Fig 5 during the fourth hour, the diameters of capacitive loop and polarization resistance values have increased and reached the highest at $1.0x10^{-4}$ M Calcein. R_p values remained unchanged at concentration higher than $1.0x10^{-4}$ M (Table 3). However, Fig 6b shows that inhibition efficiency values for all concentrations of Calcein have increased drastically after 24 h of immersion except for the $1.0x10^{-5}$ M. This could be related to the low permeability of the inhibitor film on the mild steel surface. However, after 72 h of immersion, the calculated inhibition efficiency values for the $5.0x10^{-3}$ and $1.0x10^{-3}$ M concentrations have gone as high as 99 %. These results indicate that the inhibitive action of Calcein may be related to its adsorption and thus formation of a barrier film on the mild steel surface [29].

3.4. Hydrogen evolution studies

It is well known that the spontaneous dissolution of iron in acidic medium produces Fe^{2+} ions, and it is accompanied by hydrogen evolution. This gasometric technique provides a rapid and reliable means for the assessment of the inhibitive capabilities of inhibitors on the mild steel corrosion in acidic media [30].

The volume of H_2 gas evolved from the corrosion reaction in both inhibited and uninhibited 1.0 M HCl solution as a function of exposure time during 120 hours is shown in Fig 7. As can be seen, the rate of H_2 evolution was small at the beginning of the reaction; However, as the reaction proceeded a remarkably increase was observed due to the increased surface area of the mild steel caused by the excess iron dissolution. In the presence of Calcein molecule, the rate of H_2 evolution has considerably reduced compared to the aggressive media (Fig 7). After 120 hours of immersion, 91.2 $mL.cm^{-2}$ of H_2 gas has evolved in acidic solution, whereas only 1.0 $mL.cm^{-2}$ of hydrogen gas has evolved when 1.0×10^{-3} M of Calcein was added to the acidic solution. This is due to the strong adsorption of the inhibitor molecules onto the mild steel surface and thus preventing the electrochemical reaction by decreasing the available surface area. This observation is similar to that reported in literature [31] and is

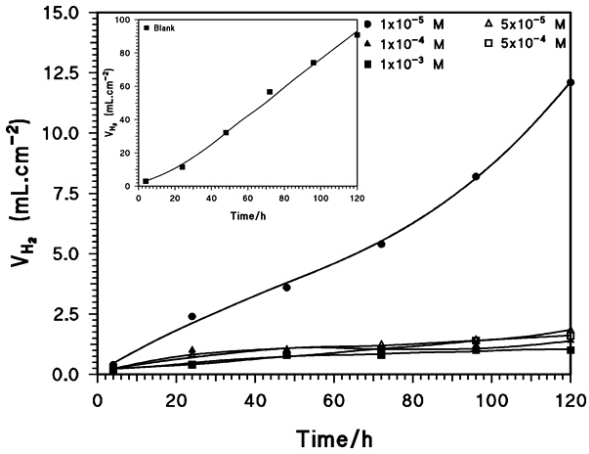

in agreement with the rest of electrochemical test results.

Figure 7: The change of hydrogen gas evolution on the mild steel electrode with exposure time in the absence and presence of various Calcein concentrations.

3.5. Effect of temperature

In order to obtain more information about the effectiveness of the inhibitor on mild steel electrode in pure 1.0 M HCl and with acid containing various concentrations of Calcein, polarization and EIS experiments were performed at temperatures ranging from 293 K to 323 K .

3.5.1. Evaluation of electrochemical impedance spectrum and linear polarization resistance values containing Calcein molecule at various temperature.

Nyquist plots of mild steel in the absence and presence of $1.0x10^{-5}$ M to $1.0x10^{-3}$ M Calcein at 293 K, 303 K, 313 K and 323 K are given in Fig 8 and Table 4.

Fig 8 shows that the diameter of the semicircles of Nyquist plots were larger in the presence of inhibitor molecule while they were smaller in the absence of calcein at the temperatures given above which is due to the increase of ionic conductivity with increasing temperature.

The R_p values have decreased from 32.5 Ω to 3.28 Ω in the absence of Calcein at elevated temperatures (293 K-323 K) as shown in Table 4. R_p values for the mild steel in 1.0 M HCl containing various concentrations of Calcein were higher than that of the blank solution at all temperatures (Fig 8). Dissolution rate of the mild steel in acidic solution is limited to concentrations higher than $5.0x10^{-5}$ M Calcein. The inhibition efficiency values for the mild steel have increased with increasing temperature. The percentage inhibition efficiency values of Calcein have increased to 88% at $1.0x10^{-4}$ M and 92% at $5.0x10^{-4}$ M respectively. The temperature increase brought about capacitance increase due to the decrease in adsorption layer thickness [32].

Linear polarization resistance measurements showed that inhibition efficiencies values obtained under the same conditions used in this study were in good agreement with those recorded from electrochemical impedance method (Table 4).

3.5.2. Evaluation of potentiodynamic polarization measurements containing Calcein molecule at various temperatures

Potentiodynamic polarization curves of the mild steel in 1.0 M HCl solution with various concentrations of Calcein were measured at temperatures ranged from 293 K to 323 K and the recorded data are presented in Fig 9. The related electrochemical parameters; corrosion potential (E_{cor}), corrosion current density (i_{cor}), cathodic Tafel slopes (β_c) and inhibition efficiency (*IE%*) values

were calculated from these curves and are listed in Table 5.

Table 4: Impedance and polarization parameters for the corrosion of the mild steel in 1.0 M HCl without and with various concentration of Calcein.

Concentration (M)	Temperature (K)	R_s	CPE $Q(x10^6 s^n \Omega^{-1})$	a	R_p	IE%	R_{ipr}	*IE%
1.0 M HCl	293	1.5	398	0.892	32.5	-	32.4	-
	303	1.1	756	0.870	20.6	-	17.6	-
	313	1.1	1300	0.869	7.43	-	9.10	-
	323	0.9	2506	0.843	3.28	-	2.90	-
$1.0x10^{-5}$	293	1.2	261	0.840	115	72	106	69
	303	1.1	851	0.805	42.5	52	42.0	58
	313	1.0	1287	0.767	23.5	68	21.9	58
	323	0.9	1507	0.783	11.1	70	9.70	70
$5.0x10^{-5}$	293	1.2	226	0.819	182	82	179	82
	303	1.0	744	0.755	89.5	77	86.3	80
	313	0.9	1132	0.755	41.3	82	41.5	78
	323	0.9	1270	0.749	23.3	86	20.6	86
$1.0x10^{-4}$	293	1.3	182	0.837	248	87	225	86
	303	1.0	608	0.738	123	83	120	85
	313	1.0	1113	0.737	47.2	84	40.5	82
	323	0.9	1202	0.752	31.9	88	28.0	90
$5.0x10^{-4}$	293	1.0	288	0.828	218	85	180	82
	303	1.1	623	0.733	156	87	168	90
	313	1.0	1674	0.683	56.7	87	59.5	85
	323	1.1	1111	0.736	41.4	92	38.5	92
$1.0x10^{-3}$	293	1.2	343	0.741	190	83	205	84
	303	1.0	902	0.712	135	85	147	88
	313	0.9	1720	0.667	71.8	90	81.0	89
	323	0.9	1105	0.692	43.1	92	45.1	94

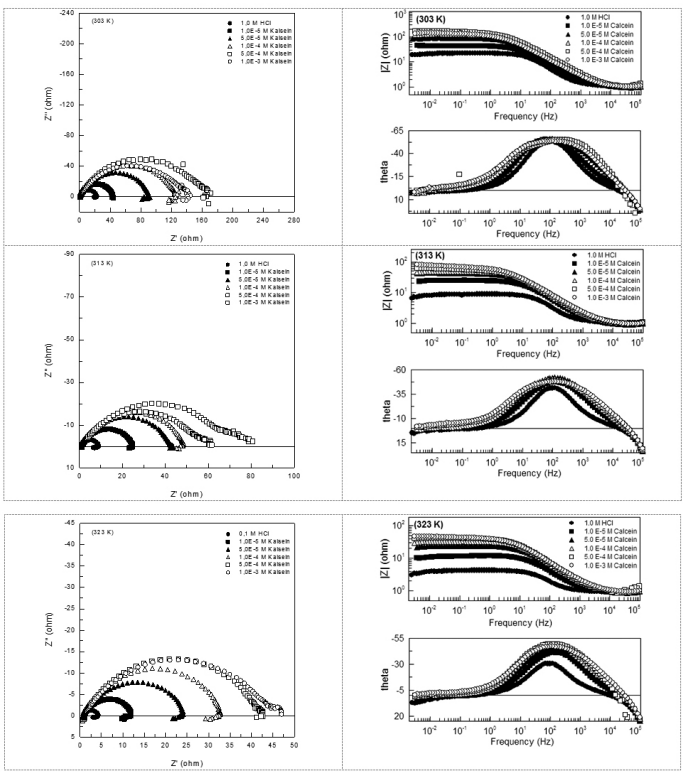

Figure 8: Nyquist and Bode plots for mild steel in 1.0 HCl solutions without and with various concentrations of Calcein at different temperatures

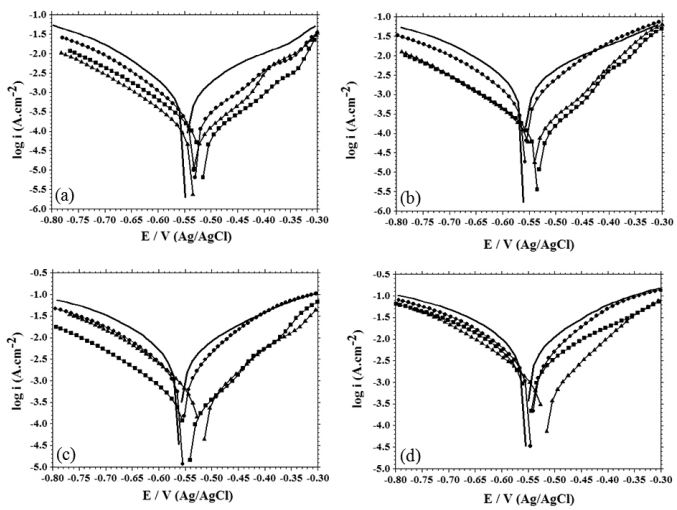

Figure 9: Anodic and cathodic polarization curves of the mild steel by Calcein in 1.0 M HCl at different temperatures (-1.0 M HCl, ● $1x10^{-5}$ M Calcein, ▲ $1x10^{-4}$ M Calcein, ■ $1x10^{-3}$ M Calcein) (a) 293 K, (b) 303 K, (c) 313 K, (d) 323 K.

From Fig 9, it is clear that both anodic metal dissolution and cathodic reduction reactions were inhibited when Calcein was added to the acid solution and this inhibition was more pronounced by increasing inhibitor concentration at all temperatures.

Table 5: Potentiodynamic polarization parameters of mild steel in the absence and presence of various concentrations of Calcein at 293-323 K.

Calcein Concentration (M)	Temperature (K)	E_{corr} (V/ Ag/ AgCl)	$-\beta_c$ (μV/ dec)	i_{corr} (μA/ cm²)	IE%
1.0 M HCl	293	-0.549	113	822	-
	303	-0.560	142	1996	-
	313	-0.561	184	5286	-
	323	-0.554	218	9504	-
$1.0x10^{-5}$	293	-0.532	103	244	70.3
	303	-0.557	127	752	62.3
	313	-0.554	145	1672	68.4
	323	-0.524	159	2864	69.9
$5.0x10^{-5}$	293	-0.525	108	140	83.0
	303	-0.548	115	282	85.9
	313	-0.533	124	676	87.2
	323	-0.521	128	1364	85.6
$1.0x10^{-4}$	293	-0.534	112	104	87.3
	303	-0.541	115	136	93.2
	313	-0.550	115	496	90.6
	323	-0.517	124	836	91.2
$5.0x10^{-4}$	293	-0.519	110	116	85.9
	303	-0.533	122	126	93.7
	313	-0.548	123	340	93.6
	323	-0.522	134	800	91.6
$1.0x10^{-3}$	293	-0.517	114	116	85.9
	303	-0.534	121	134	93.3
	313	-0.544	126	302	94.3
	323	-0.516	138	794	91.6

The increase in inhibition efficiency shows that the inhibitive film formed on the metal surface is more protective at higher temperatures, possibly because the adsorption of the inhibitor occurs together with corrosion products. The variable values of the cathodic Tafel slopes suggest that the inhibiting action of Calcein occurs by simple blocking of the electrode surface area, thus decreasing the surface area available for hydrogen evolution without affecting the reaction mechanism [12, 33].

3.6. Activation energy of metal dissolution

The activation energy for the corrosion process are calculated from Arrhenius equation [34]:

$$\ln(i_{corr}) = \ln A - \frac{E_a}{RT} \qquad (6)$$

where E_a represents the apparent activation energy, R the gas constant, A the pre-exponential factor and i_{corr} is the corrosion rate, obtained from the potentiodynamic polarization method. Arrhenius plots for the corrosion rate of mild steel are given in Fig 10.

Values of E_a for mild steel in 1.0 M HCl and in the presence of inhibitor were obtained from the slope of ln (i_{corr}) vs. $1/T$. The calculated E_a value for the blank was 65.5 kJ/mol and for those containing $1.0x10^{-5}$ M, $5.0x10^{-5}$ M, $1.0x10^{-4}$ M, $5.0x10^{-4}$ M and $1.0x10^{-3}$ M inhibitor were calculated as 64.7, 60.6, 59.2, 53.0 and 51.4 kJ/mol respectively. E_a values were found to be lower in the inhibited system. The lower value of the activation energy is attributed to the chemisorption of inhibitor on steel surface. This conclusion was in accordance with the findings of other researchers [28,35,36].

3.7. Adsorption isotherm and thermodynamic parameters of Calcein

The information on the interaction between the inhibitor molecules and the metal surface can be provided by the adsorption isotherm. The adsorption behaviour of the organic compound can be described by two main types of interaction: physical adsorption and chemisorption. These are concerned by the chemical structure of the inhibitor, the type of the electrolyte, the charge and nature of the metal. The adsorption mechanism of Calcein on the mild steel surface was determined by fitting the θ values (obtained from potentiodynamic polarization measurements) to different adsorption isotherms such as Langmuir, Frumkin, Freundlich, Temkin and Florry-Huggins for different temperatures. The best fits were obtained from Langmuir adsorption isotherm where the correlation coefficients for all temperatures were calculated as 0.997 and 0.999. According to this isotherm, θ is related to the inhibitor concentration $C_{(inh)}$.

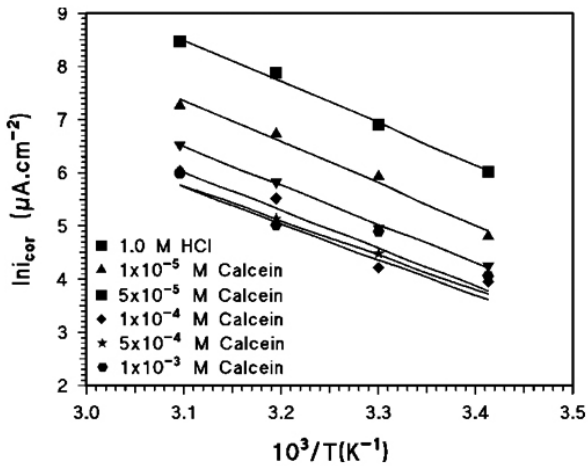

Figure 10: The relationship between ln i_{corr} and 1/T for mild steel in 1.0 M HCl in presence of Calcein.

$$\frac{C_{(inh)}}{\theta} = \frac{1}{K_{(ads)}} + C \qquad (7)$$

where $C_{(inh)}$ is the inhibitor concentration and $K_{(ads)}$ is the adsorption equilibrium constant of the adsorption process (Fig 11). The calculated $K_{(ads)}$ values are given in Table 6.

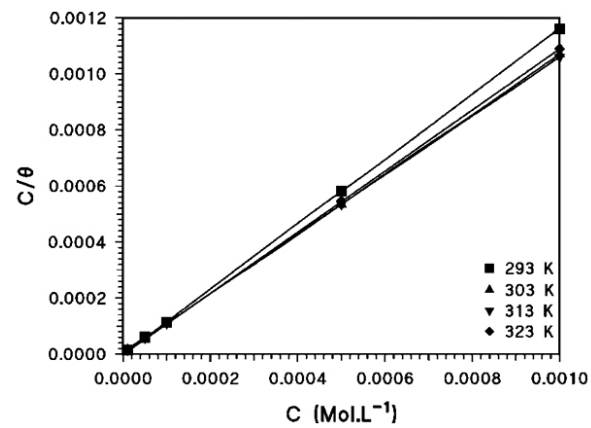

Figure 11: Langmuir isotherm plots for adsorption of Calcein on mild steel in 1.0 M HCl at different temperatures.

In our study we have calculated the adsorption free energy (DG°_{ads}) from Langmuir adsorption isotherm:

$$K_{ads} = \frac{1}{55.5}\exp\left(-\frac{\Delta G^{\circ}_{ads}}{RT}\right) \qquad (8)$$

The calculated $K_{(ads)}$ and ΔG°_{ads} values are given in Table 6.

The values of thermodynamic parameters for the adsorption of inhibitors can provide valuable information about the mechanism of corrosion inhibition. Thermodynamic adsorption parameters are known as adsorption free energy (ΔG°_{ads}), adsorption entropy (ΔS°_{ads}) and adsorption heat (ΔH°_{ads}). These parameters can be calculated by using different mathematical techniques. In our experiments the variation of adsorption free energy with temperature has given second order polynomial which was calculated by using MAPLE Software in the following equation

$$\Delta G^{\circ} = -15.850\,T^2 + 9.8170x10^3\,T - 1.5614x10^6 \qquad (9)$$

Thermodynamic model can be applied to corrosion inhibition of mild steel in the presence of Calcein molecule. Moreover, the calculated heat of adsorption and entropy of adsorption values can be better explained. The most common independent variables are T and P and from Gibbs equations we can obtain temperature dependences of free energy, G; which is expressed as;

$$dG = -SdT + VdP \qquad (10)$$

At constant pressure, $dP = 0$ therefore ΔS_{ads} can be obtained from equation (11).

$$\Delta S^{\circ} = -\left(\frac{dG}{dT}\right)_p \qquad (11)$$

Second order polynomial expression was obtained and by substituting the G and T values in (11) and thus $-\Delta S^{\circ}_{ads}$ was obtained from this equality. Adsorption entropy values were calculated from equation (12) at all of temperatures studied

$$\Delta S^{\circ} = 31.700\,T - 9.8170x10^3 \qquad (12)$$

ΔH°_{ads} values at all temperatures studied were calculated from the basic thermodynamic equation.

$$\Delta G^{\circ}_{ads} = \Delta H^{*} - T\Delta S^{\circ}_{ads} \qquad (13)$$

Since Gibbs-Helmholtz equation is expressed as

$$\left(\frac{d\left(\Delta G^{\circ}_{ads}/T\right)}{dT}\right)_p = -\frac{\Delta H^{\circ}_{ads}}{T^2} \qquad (14)$$

The relationship can be written as:

$$\int d\left(\frac{\Delta G^{\circ}_{ads}}{T}\right) = -\int \frac{\Delta H^{\circ}_{ads}}{T^2} dT \qquad (15)$$

And the following equation can be obtained:

$$\frac{\Delta G^{\circ}_{ads}}{T} = \frac{\Delta H^{\circ}_{approx}}{T} + C \qquad (16)$$

Constant (C) values at all temperatures studied were calculated from Equation 16 by substituting the adsorption free energy and the enthalpy values calculated form Eq. 13.

When polynomial Eq. (9) was substituted into eq. 16, eq.17 was obtained and the resultant adsorption heat energy (ΔH°_{ads}) were calculated from this equation:

$$\frac{-15.850\,T^2 + 9.8170x10^3\,T - 1.5614x10^6}{T} = \frac{\Delta H^{\circ}_{ads}}{T} + C \qquad (17)$$

All thermodynamic adsorption parameters for Calcein on mild steel in 1.0 M of HCl solution are listed in Table 6.

Table 6: The thermodynamic parameters of adsorption process obtained from the impedance data by applying Langmuir isotherm for mild steel in 1.0 M HCl solution containing various concentrations of Calcein at different temperatures.

T (K)	K_{ads}	ΔG°_{ads} (kJ/mol)	ΔS°_{ads} (J/molK)	ΔH°_{ads} (kJ/mol)
293	$2.50x10^6$	- 45.6706	-529	-109
303	$3.33x10^5$	- 42.1509	-212	-22
313	$1.43x10^5$	- 41.3424	105	-8
323	$2.50x10^5$	- 44.1634	422	92

Generally, values up to -20 kJ/mol of ΔG°_{ads} are electrostatic interaction between the charged molecules and the charged metal (physisorption) while those around -40 kJ/mol or higher are associated with chemisorption that results from sharing or transferring electrons from the inhibitor molecules to the metal surface to form a coordinate type of bonding [37]. As can be seen from Table 6, at all temperatures studied Calcein shows slightly higher negative ΔG° values than -40 kJ/mol which indicate chemical adsorption whose contribution to the adsorption phenomenon probably was low at 25 °C and increased with temperature. Chemisorption could occur interaction of the unshared electron pairs of nitrogen and oxygen atoms with the d-orbitals of iron atom to provide a protective chemisorbed film [38].

The adsorption of Calcein onto the mild steel surface at low temperatures is an exothermic process and endothermic at high temperatures. In the exothermic process (ΔH°_{ads}<0), negative heat of adsorption may be due to physisorption, chemisorption or both. Physisorption is distinguished from chemisorption where, ΔH°_{ads} for the physisorption process are lower than 40 kJ.mol^{-1} while for chemisorption it can increase to 100 kJ.mol^{-1}. However, an endothermic process (ΔH°_{ads}>0), it is entirely attributed to chemisorption [39]. In the present study, the effect of temperature on the performance of the Calcein clearly indicates that the inhibition efficiency values have increased with increasing temperature (Table 5). This behavior can be explained by the specific interaction between mild steel surface and inhibitor molecule as reported in the literature [40,41]. The calculated values of the ΔH°_{ads} for the adsorption of Calcein have showed chemisorptions at the studied temperature range. It is also clear that ΔS°_{ads} values (-109, -22, -8 and 92 J/mol.K for 293 K, 303 K, 313 K and 323 K) have increased positively with increasing temperature.

3.8. UV-visible analyis

The absorption of monochromatic light is a suitable method for identification of complex compounds. The change in the position of absorption maximum or change in the value of absorbance indicates the formation of a complex between the two species in solution [42]. However, In order to verify the possibility of complex formation between the inhibitor and iron, UV-visible absorption was measured for both the inhibitor and for mild steel treated with inhibitor for 120 h (Fig 12).

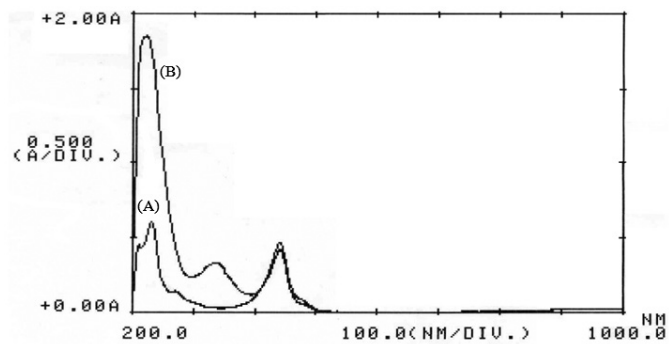

Figure 12: Uv-visible spectra of the solution containing 1.0 M HCl in $1x10^{-5}$ M Calcein before (Curve A) and after (Curve B) mild steel immersion.

Bands at 231 and 441 nm are attributed to the π - π^* and n - π^* transitions of the carbonyl group which is present in Calcein (Curve A). The band in the region 339 nm, indicates that the carbonyl groups are held up in the complex with iron (Curve B). This conclusion displays an evidence for the formation of

a complex between Fe^{2+} and Calcein in 1.0 M HCl solution.

3.9. Surface Morphology

Micrograph was recorded to establish the interaction of organic molecules with the metal surface. The surface images, which show the features of mild steel surface after immersion in 1 M HCl for 120 h in the absence and presence of $1.0x10^{-5}$ M, $1.0x10^{-4}$ M and $1.0x10^{-3}$ M Calcein are shown in Fig 13.

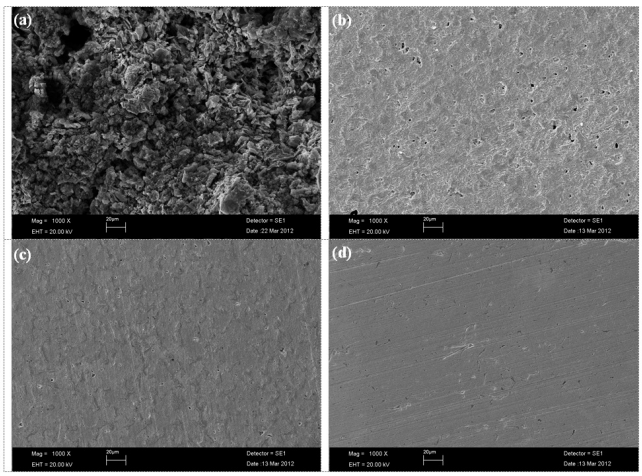

Figure 13: SEM micrographs of (a) blank and (b) $1x10^{-5}$ M, (c) $1x10^{-4}$ M and (d) $1x10^{-3}$ M Calcein in 1.0 M HCl solution after immersion of 120 h.

The metal surface immersed in 1.0 M HCl was rough, full of metal imperfections such as pits, cavities, voids and cracks. These are essentially due to the corrosion products on the metal surface. Surface micrographs of the specimens immersed in the Calcein solutions (Fig 13 b, c and d) were in much better conditions having polished and smooth surfaces. This is due to the formation of a protective film that has hindered the dissolution of mild steel surface especially in the $1.0x10^{-3}$ M Calcein. The electrochemical and surface micrograph results were in good agreement with each other.

3.10. Mechanism of inhibition

Adsorption is a key process in the explanation of inhibition mechanism where, it may suggest that inhibitor molecules are adhered to the metal surface, that decreases the surface area on which cathodic and anodic reactions took place [43]. These reactions are associated with the chemical structure of the inhibitor molecule [44]. Four types of adsorptions: *(i)* electrostatic attraction between charged molecules and the charged metal, *(ii)* interaction of π-electrons with the metal, *(iii)* interaction of uncharged electron pairs in the molecule with the metal and *(iv)* a combination of the above [45] may have taken place at the metal solution interface in the aggressive acidic media.

Corrosion inhibition of mild steel in hydrochloric acid solution by Calcein is based on molecular adsorption. Calcein slows down corrosion rate of mild steel by controlling both the anodic and cathodic reactions. Anodic dissolution of mild steel decreases by the adsorption of Calcein molecule. This is attributed to the abundance of p electrons and the interaction of unshared electron pairs of nitrogen and oxygen atoms with the vacant d-orbital of iron. At the same time, since Calcein molecule is present in a protonated form in the acidic solution, it is adsorbed on the cathodic sites of the mild steel and therefore decreases the evolution of hydrogen.

The lower values of E_a in presence of the Calcein and higher negative values of ΔG^o_{ads} (-40 kJ.mol^{-1}) in all Calcein concentrations studied are interpreted as an indication to chemical adsorption. However, by increasing the temperature, some chemical changes may have occurred in the inhibitor molecules, leading to an increment in the electron densities at the adsorption centers of the molecule, and thus causing an improvement in inhibitor efficiency [46]. The increase of *IE%* with temperature due to specific interaction between the inhibitor molecule and the mild steel surface and can be also explained by the change in the adsorption character where, at a low temperatures it is physical and transforms into chemical by its increase [28, 47]. This interpretation is also supported by the UV-vis analysis.

4. CONCLUSIONS

From this study the following conclusions are drawn:

1. Calcein molecule is a good inhibitor for mild steel corrosion in 1.0 M hydrochloric acid solution. The results obtained from the impedance, potentiodynamic polarization and linear polarization resistance techniques indicated that the increase in the concentration of Calcein have improved the inhibitor efficiency for short time immersions.

2. The slightly positive shift in the corrosion potentials and decrease in the anodic and cathodic current densities in the presence of Calcein suggested that these compounds can act as mixed type inhibitor with predominant control of anodic reaction.

3. Inhibition efficiency increases at elevated temperatures.

4. The impedance measurements at E_{corr} showed two capacitive loop which is related to the dielectric properties of the surface film. Increasing the polarization resistance R_p values by increasing the concentration of Calcein shows that inhibition ability of the compound depends on the adsorption of the molecule on mild steel surface.

5. EIS measurements over extended immersion periods showed that higher inhibitor concentration and longer exposure of mild steel to Calcein have lead to increase in inhibition efficiency.

6. The adsorption of Calcein on mild steel surface was found to be spontaneous and obeys Langmuir adsorption isotherm.

7. The values of kinetic/thermodynamic parameters (E_a, ΔG^o_{ads}, ΔH^o_{ads}) have suggested the existence of chemical adsorption.

8. The UV-Vis studies clearly reveal the formation of complex that is responsible for the observed inhibition.

9. Micrographs and hydrogen evolution studies have confirmed these results.

ACKNOWLEDGMENT

The authors are grateful to Nigde University and Osmaniye Korkut Ata University for their support.

REFERENCES

1. E.A. Noor, A.H. Al-Moubaraki, **Mater. Chem. Phys. 110**, 145. (2008).
2. I.B. Obot, N.O. Obi-Egbedi, **Curr. Appl. Phys., 11,** 382, (2011).
3. S.S. Abd El Rehim, S.M. Sayyah, M.M. El-Deeb, S.M. Kamal, R.E. Azooz, **Mater. Chem. Phys. 123**, 20 (2010).
4. H. Keleş, M. Keleş, I. Dehri, O. Serindağ, **Colloid. Surf. 320,** 138, (2008).
5. E. Bayol, A.A. Gürten, M. Dursun, K. Kayakırılmaz, **Acta Phys.Chim. Sin. 24,** 2236, (2008).
6. M. S. Eswaran, P. K. Mathur, **Corros. Sci. 38,** 1783, (1996).
7. A. Lecante, F. Robert, P.A. Blandinières, C. Roos, **Curr. Appl. Phys. 11,** 714, (2011).
8. A. Y. Musa, A. A. H. Kadhum, A. B. Mohamad, M. S. Takriff, E. P. Chee, **Curr. Appl. Phys. 12,** 325, (2012).
9. M.A. Quraishi, S.K. Shukla, Mater. **Chem. Phys. 113,** 685, (2009).
10. S. Issaadi, T. Douadi, A. Zouaoui, S. Chafaa, M.A. Khan, G. Bouet, **Corros. Sci. 53** 1484, (2011).
11. Ishtiaque Ahamad, Rajendra Prasad, M.A. Quraishi, **Corros. Sci. 52,** 1472, (2010).
12. M.A. Qurashi, D. Jamal**, Mater. Chem. Phys. 78,** 608, (2003).
13. Y. Sürme, A.A. Gürten, **Corros. Eng. Sci. Techn. 44,** 3004, **(**2009).
14. M.S. Morad, A.A.O. Sahran, **Corros. Sci. 50,** 744, (2008).
15. J. Aljourani, K. Raeissi , M.A. Golozar, **Corros. Sci. 51,** 1836, (2009).
16. M. Behpour, S.M. Ghoreishi, N. Soltani, M. Salavati-Niasari, **Corros. Sci. 51,** 1073, (2009).
17. M. Erbil, **Chim. Acta Turc. 1,** 59, (1988).
18. T. Tüken, B. Yazıcı, M. Erbil, **Turk. J. Chem., 26,** 735, (2002).
19. G. Kardaş, R. Solmaz, **Corros. Rev. 24,** 151, (2006).
20. R. Solmaz, G. Kardas, B. Yazıcı, M. Erbil, **Colloid. Surfaces A 312,** 7, (2008).
21. M. E. Orazem, N. Pébère, B. Tribollet, **J. Electrochem. Soc. 153 (4)**, B129, (2006).
22. B. Hirschorn, M. E. Orazem, B. Tribollet, V. Vivier, I. Frateur, M. Musiani, **Electrochim. Acta 55**, 6218, (2010).
23. M. Ozcan, I. Dehri M. Erbil, **Prog. Org. Coat. 44,** 279, (2002).
24. F. Bentiss, M. Lebrini, H. Vezin, F. Chai, M. Traisnel, M. Lagrené, **Corros. Sci. 51,** 2165, (2009).
25. H. H. Hamdy, E. Abdelghani M.A. Amin, **Electrochim. Acta 52,** 6359, (2007).
26. M. Nobial, O. Devos, O. R. Mattos and B.Tribollet, **J. Electroanal. Chem. 600,** 87-94, (2007).

27. M.Ozcan, I. Dehri, M. Erbil, **Appl. Surf. Sci. 236,** 155, (2004).
28. F. Mansfeld, **J. Appl. Electrochem. 25,** 187, (1995).
29. M.A. Quraishi, S. K. Shukla, Mater. **Chem. Phys. 113,** 685, (2009).
30. S.S. Abdel Rehim, O.A. Hazzazi, A.A. Mohammed, F.F. Khaled, **Corros. Sci. 50**, 2258, (2008).
31. O. N. Eddy, E. E. Ebenso, U. J. Ibok, E. E. Akpan, **Int. J. Electrochem. Sci., 6,** 4296, (2011).
32. A. Popova, **Corros.Sci. 49,** 2144, **(**2007).
33. M.M. Osman, R.A. El-Ghazawy, A.M. Al-Sabagh, Mater. **Chem. Phys. 80,** 55, (2003).
34. X. Li, S. Deng, G. Mu, H. Fu, F. Yang, **Corros. Sci. 50,** 420, (2008).
35. M. S. Morad A. M. Kamal El-Dean, **Corros. Sci. 48,** 3398, (2006).
36. F.S. de Souza, A. Spinelli, Caffeic **Corros. Sci. 51,** 642, (2009).
37. S.A. Ali, A.M. El-Shareef, R.F. Al-Ghamdi, M.T. Saeed**, Corros. Sci. 47,** 2659, (2005).
38. X. Li, S. Deng, H. Fua, T. Li, **Electrochim. Acta 54,** 4089, (2009).
39. A. N. Ehteram, A. H. Al-Moubaraki, Mater**. Chem. Phys. 110,** 145, (2008).
40. S.V. Ramesh, A.V. Adhikari, Mater**. Chem. Phys. 115,** 618, (2009).
41. Y.P. Khodyrev E. S. Batyeva E. K. Badeeva, E. V. Platova, L., Tiwari, O. G. Sinyashin **Corros. Sci. 53,** 976, (2011).
42. N.O. Obi-Egbedi, K. E. Essien, I. B. Obot, E. E. Ebenso, **Int. J. Electrochem. Sci., 6,** 913, (2011).
43. A.J. Bard, L.R. Faulkner, Electrochemical Methods, John Wiley and Sons, New York, p. 517, 1980.
44. H.L. Wang, H.B. Fan, J.S. Zheng, **Mater. Chem. Phys. 77,** 655, (2002).
45. D. Schweinsgberg, G. George, A. Nanayakkawa and D. Steinert, **Corros. Sci., 28,** 33, (1988).
46. A.K. Satpati, P.V. Ravindran**, Mater. Chem. Phys. 109,** 352, (2008).
47. M. Abdallah, **Corros. Sci. 44,** 717, (2002).